UNIVERSITÄT HEIDELBERG
ZUKUNFT SEIT 1386

Universität Heidelberg
Fortgeschrittenen-Praktikum

F61 Nuclear magnetic resonance

Long Report

Nils Schmitt Timo Kleinbek

Conducted in August 2018
Supervisor: Minjung, Kim

Abstract

In this experiment we started by studying the basics of magnetic excitation. In particular, we wanted to understand how exactly nuclear spins are excited to perform Larmor precession. We measured the relaxation time in the first part of the experiment. In the second part, we identified different substances by comparing the measured shifts of the Larmor frequency caused by different molecular structures. Lastly, we used nuclear magnetic resonance and different imaging methods to take pictures of several objects, analogously to the medical MRI treatment.

Contents

1. Theoretical Basics

Basics and the relaxation time

In an applied external magnetic field, existing magnetic moments of the atomic nuclei in a material align themselves along the external magnetic field, parallel or anti-parallel. The corresponding energy splitting is given by the scalar product of magnetic moment and external magnetic field in the form

$$\Delta E = -\boldsymbol{\mu} \cdot \boldsymbol{B}_0. \tag{1}$$

The parallel alignment is energetically lower.
The proton population numbers correctly described by the Fermi-Dirac statistics can be approximated classically by the Boltzmann distribution. The ratio of the two occupation numbers with parallel and antiparallel alignment is then given by

$$\frac{N_+}{N_-} = \mathrm{e}^{\frac{2\Delta E}{k_\mathrm{B} T}}. \tag{2}$$

An estimate in which the magnetic moment is approximately one Bohr's magneton and the magnetic field is approximately 1 T results in a difference between the two occupation numbers of approximately one per thousand at room temperature.
The total magnetization results from the sum of these thousandth part over the whole substance. In general, the following applies from the electrodynamics for the resulting torque from a magnetic field and a magnetization

$$\boldsymbol{\tau} = \boldsymbol{M} \times \boldsymbol{B}_0. \tag{3}$$

For (anti-)parallel alignment, the torque is zero. As soon as B_0 and M span a plane, the resulting torque rotates the magnetization around the axis of the magnetic field with the Larmor frequency

$$\omega_\mathrm{L} = \gamma\, B_0. \tag{4}$$

Now we create a second magnetic field B_1 orthogonal to a relatively strong external magnetic field B_0. Before the magnetization can align itself along the new total magnetic field B_tot, the Larmor precession around this begins. If the magnetic field B_1 oscillates with the Larmor frequency of the atomic nuclei, the magnetization can be deflected, as schematically shown in Figure 1. With the

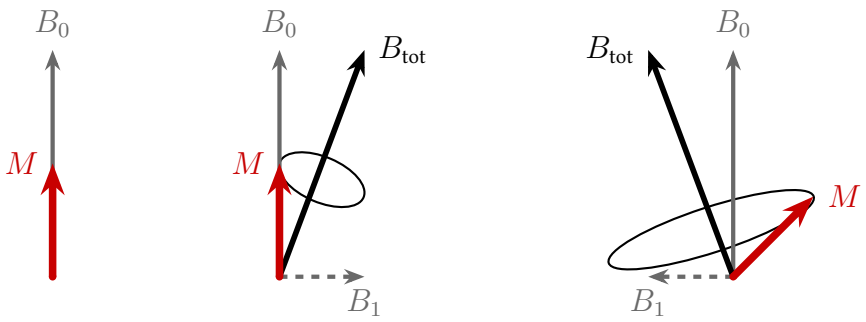

Figure 1: High-frequency external magnetic field generates elongation of magnetization.

duration of the applied high-frequency magnetic field B_1 we can determine the angle by which the magnetization is deflected compared to the external magnetic field B_0. In particular, so-called 90° and 180° pulses can be generated, which generate an orthogonal or antiparallel magnetisation to B_0 from a parallel magnetisation.

For these excited states of magnetization, the Bloch equations result in an asymptotic drop on characteristic time scales for antiparallel and orthogonal magnetization respectively T_1 and T_2:

$$M_\parallel(t) = M_0 \cdot \left(1 - 2\mathrm{e}^{-\frac{t}{T_1}}\right) \tag{5}$$

$$M_\perp(t) = M_0 \cdot \mathrm{e}^{-\frac{t}{T_2}} \tag{6}$$

The decay of the anti-parallel magnetization is caused by the interaction of the spins with the external magnetic field B_0 (spin-grating changer effect), whereas interactions between the individual spins (spin-spin interaction) lead to the decay of the parallel magnetization. Since the spin-spin interaction is stronger than the spin-grating interaction, $T_2 \leq T_1$ is expected.
Measurements of orthogonal magnetization are made in the B_1 generating coil by induction. After switching off the B_1 field, the precession of the magnetization around the external magnetic field B_0 induces an alternating current in the B_1 coil. This can be measured on a connected oscilloscope. In our setup, the output signal of the induction coil leads back again into the signal generator, which generates the high-frequency alternating field B_1, and only then into the readout devices. Thus we see the final signal as a superposition of the signal frequency and the alarm frequency, which shows the sum and difference of the two frequencies. We also call the difference the operating frequency, which is a few hundred hertz; this difference is in the per thousand range relative to the larmor frequency of hydrogen nuclei (about 20 MHz).

The relaxation time T_1 can be measured by first passing a 180° pulse an antiparallel orientation of the magnetization is caused and then after different time intervals a 90° pulse generates a signal in the induction coil whose amplitude is proportional to the magnitude of the antiparallel magnetization of before the 90° pulse. By recording these amplitudes after different times, the exponential decrease of the antiparallel magnetization can be investigated and T_1 determined.

The relaxation time T_2 is measured by another combination of 90° and 180° pulses. First a 90° pulse produces a magnetization perpendicular to the B_0 field, which because of this field begins to precisionize this axis with the Larmor frequency. However, the external magnetic field is designed so that the magnetic field strength varies in the direction of the magnetic field vector.ends on it, the frequency at different coordinates is also different, which after a certain time results in a phase diff Because the Larmor frequency by equation 4 deperence at the different coordinates. This incoherence reduces the amplitude of the induced field in the coil. After a certain period of time τ a 180° pulse is sent, which causes a mirroring around 180° on an axis perpendicular to the axis of the B_0 field around which the magnetization rotates. The consequence of this mirroring is that the nuclei that were previously in phase after the other nuclei are now at the same phase angle in front of them. The previous phase difference was due to the precession during a time τ had arisen. By mirroring through the 180° pulse, after a further precession period of τ, the nuclei are all in phase again and thus show a maximum induction current. This allows the magnitude decrease to be measured over a period of 2τ .
Now you can always use different values for τ and measure the decrease of the amplitude after twice the time to reconstruct the exponential decrease and so T_2. This measuring method is called spin-echo method.

Alternatively, another 180° pulse can be sent to all odd multiples of time τ so that a maximum induction current is measured at all even multiples of τ and the relaxation time can be determined from this. This sequence of one 90° and several 180° pulses is called the Carr-Purcell sequence. The basic procedure of the process described here is shown in figure 2 is illustrated.

Chemical Shift

When considering the excitation of nuclear spins, only atoms that actually have a nuclear spin can be excited (i. e. $S \neq 0$). Of course, a single proton as fermion in the nucleus of a hydrogen atom has

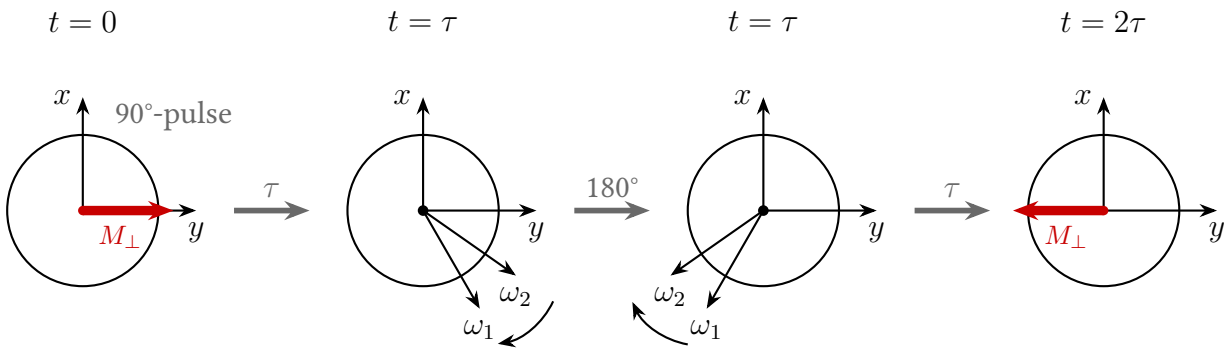

Figure 2: Diagram for measuring the relaxation time T_2.

a spin of $S = 1/2$. On the other hand, for a carbon atom, for example $S = 0$, so there is no magnetic moment at all that could contribute to magnetization.
Additionally, note that the 90° and 180° pulses are always adjusted to a noise frequency. In order to achieve an effective excitation of nuclear spins of different atoms, the gyromagnetic ratio must also be the same. If we expose a sample of organic material to only one frequency that excites hydrogen nuclei, only the hydrogen atoms of an organic material will contribute to the measured larmor frequency. In different molecules the hydrogen molecules are present in different bonds with different electronegativity differences, which means that the probability of residence of the electrons around the proton is not always the same. Due to this difference, the externally applied magnetic field B_0 is also shielded to different degrees by the electron, which results in a slightly different larmor frequency. The shielded part of the magnetic field is described by

$$\delta \boldsymbol{B} = -\sigma \boldsymbol{B}_0, \tag{7}$$

where σ is the proportionality factor. For a certain material, the changed Larmor frequency results accordingly from the superposition of both magnetic fields to

$$\omega_i = \omega_\mathrm{L}(1 - \sigma_i). \tag{8}$$

In order to identify a sample on the basis of this shift of the Larmor frequency, the shielding factors relative to a reference sample (here Tetra-Methyl-Silane, short TMS) are measured by measuring the distance of the corresponding resonance peaks. This distance then corresponds to

$$\delta_i \cdot \omega_\mathrm{L} = \omega_\mathrm{TMS} - \omega_i. \tag{9}$$

The differences of the shielding factors $\delta_i = \sigma_i - \sigma_\mathrm{TMS}$ can then be looked up in a table as shown in figure 3.
The positions of the molecules in this list can be explained using the example of a COOH group. Here, the hydrogen atom is directly bonded to an oxygen atom with a relatively high electronegativity, while a second oxygen atom is bonded directly to an oxygen atom with a relatively high electronegativity. oxygen atom is still in the immediate vicinity. The hydrogen atom itself is thus virtually "naked" and is hardly shielded from its electron, which leads to a stronger effective magnetic field compared to C-H bonds and thus to an increased larmor frequency.

Imaging Techniques

By excitation of nuclear spins and subsequent measurement of the magnetization, the distribution of the excited spins can be reconstructed under certain conditions and thus one-, two- or three-dimensional images of the nuclear spin distribution can be generated. To divide the material into

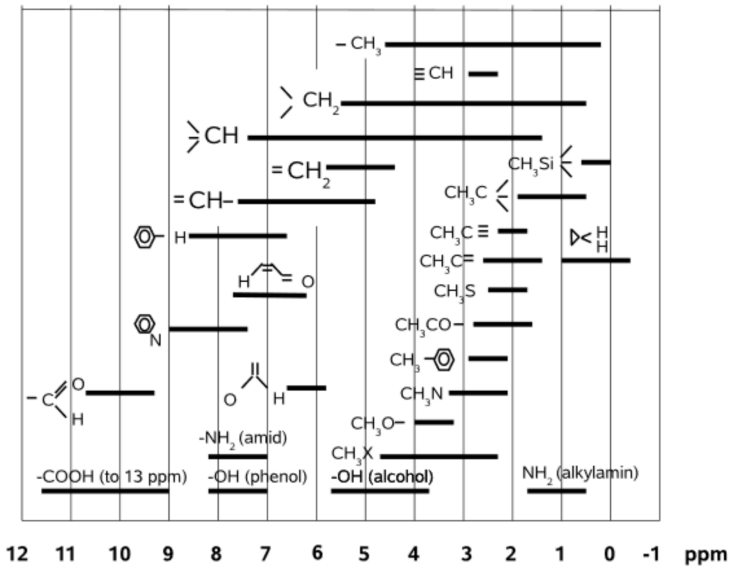

Figure 3: Chemical shifts of different molecules relative to TMS [1].

readable pixels in the different dimensions, in addition to an external B_0 field along the direction, which we now define as z direction, we use magnetic fields, which also point in z direction but change spatially with the x, y or z coordinate. In x direction, for example:

$$\boldsymbol{B}_x = (0, 0, G_x x)$$

Frequency Coding

After equation 4 the Larmor frequency in a magnetic field, which is superimposed by B_0 and a field varying in z direction, results to

$$\omega_{\mathrm{L}}(z) = \gamma(B_0 + G_z z) = \omega_{\mathrm{L}}^0 + \omega_z. \tag{10}$$

As soon as a 90° pulse causes a magnetization in the $x - y$ plane, this precedes the z position with different alarm frequency around the axis of the magnetic field. The signal generated in an adjacent induction coil whose axis must be perpendicular to the z direction is then proportional to the sum of all magnetizations multiplied by the phase resulting from the high frequency of the 90° pulse

$$S(t) \sim \int_V M_\perp(z,t)\, \mathrm{e}^{-\mathrm{i}\omega_{\mathrm{HF}} t}\, \mathrm{d}V \tag{11}$$

what is equal to

$$S(t) \sim \int_V M_\perp^{\mathrm{rot}}(z,t)\, \mathrm{e}^{-\mathrm{i}\left(\omega_{\mathrm{L}}^0 + \omega_z - \omega_{\mathrm{HF}}\right) t}\, \mathrm{d}V\,. \tag{12}$$

If we assume that $\Omega = \omega_{\mathrm{L}}^0 - \omega_{\mathrm{HF}}$, the exponential function before the integral only contributes a phase and we get

$$S(t) \sim \mathrm{e}^{\mathrm{i}\Omega t} \int_Z \left(\int_X \int_Y M_\perp^{\mathrm{rot}}(z,t)\, \mathrm{d}y\, \mathrm{d}x \right) \mathrm{e}^{\mathrm{i}\omega_z t}\, \mathrm{d}z\,. \tag{13}$$

After integration over the area of the induction coil, the measured signal is thus proportional to the Fourier transform of the magnetization. By measuring the signal at different times t_i the distribution of the magnetization depending on the position z can be calculated by discrete Fourier transformation. As usual for functions that are linked via Fourier transform, the product of characteristic widths of the functions is constant.
Therefore, the following applies

$$\Delta z \sim \frac{1}{\Delta t}. \tag{14}$$

The nuclear spins along the z coordinate have because of the inhomogeneous magnetic field different Larmor frequencies and the information of the position is "encoded" by these frequencies. Therefore we also call this method frequency coding.
For the resolution of a two-dimensional image we cannot simply use a apply inhomogeneous magnetic field in an additional direction because the two fields would superimpose each other and the magnetization would occur along the corresponding diagonals. Rather, we need a second type of coding, which we find in phase coding.

Phase Coding

By applying an inhomogeneous magnetic field and the different Larmor frequency, a phase difference

$$\Delta\phi(z) = \phi(z) - \phi(0) = \gamma G^z z t = \omega_z t \tag{15}$$

between the nuclear spin. If we create such a field for a fixed time T_{Ph}, the phase is dependent on the z-coordinate in the form

$$\phi(z) = \gamma G^z T_{\text{Ph}} z = k_z z. \tag{16}$$

Similar to the steps above, signal and magnetization are again linked via Fourier transformation. Instead of creating several measuring points over time, different in the phase coding, the k_z implicitly defined above is obtained by varying the magnetic field gradient or the action time and thus receive a collection of measuring points that can be transformed back.

Two dimensional imaging

As already mentioned, we now use both of the coding possibilities mentioned to create two-dimensional images. For a three-dimensional sample, we must first select a thin layer from which we want to generate the two-dimensional image. This selection is made by selective excitation of the nuclear spins in the layer to be examined. In a magnetic field gradient, for a layer whose z coordinate is between z_1 and z_2, the Larmor frequencies are also between corresponding frequencies ω_1 and ω_2. The transmission of a square-wave signal in the frequency space between these frequencies allows selective excitation of the desired layer.
Then the nuclear spins can be encoded one after the other in the two dimensions as illustrated in figure 4. In a first step, by applying an inhomogeneous magnetic field in x direction, different phases can be assigned to the spins in x direction, which are retained after switching off the additional inhomogeneous field, because then all spins again further precise with the same alarm frequency. In the last step, an inhomogeneous field is created in the y direction and the y direction is encoded in

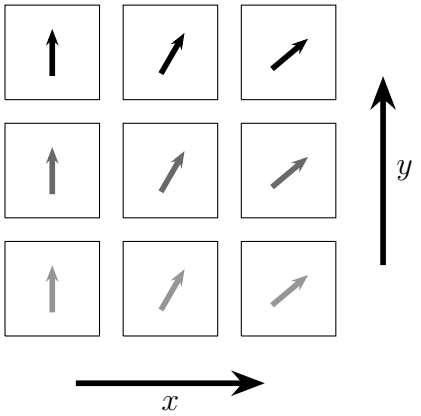

Figure 4: Spins for two-dimensional images, where the direction of the arrow symbolizes the phase and the grayscale the frequency.

different frequencies. Here a data set is recorded directly in a certain time interval. To scroll through the pixels in the x direction, the k_z must be changed again. This produces a two-dimensional data set, which is again transformed into an image by two-dimensional inverse Fourier transformation. of the magnetization can be translated. The procedure of this data acquisition is shown in figure 5. It is obvious that by stimulating individual layers and creating the respective images one after the

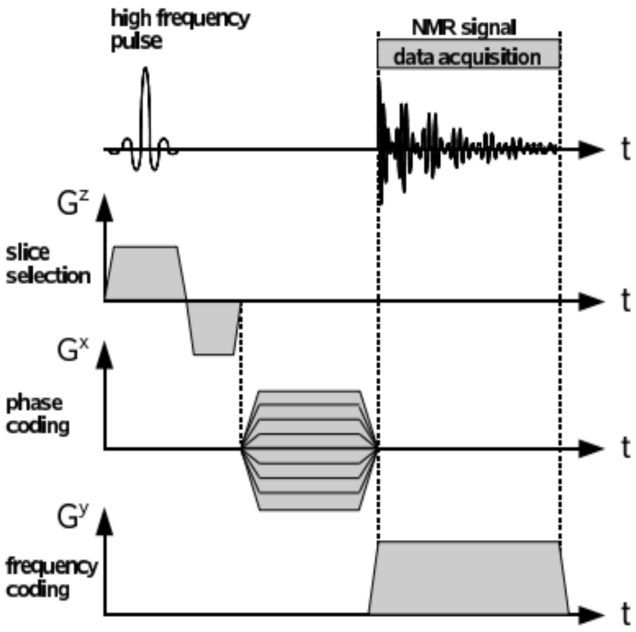

Figure 5: Datarecording for two dimensional imaging [1].

other, three-dimensional objects can also be examined.

2. Measurements Log and Evaluation

Experimental setup

The relaxation times and the chemical shift were measured with a Bruker minispec p20 (see fig. ??). The arrangement is divided into the p20 electrical unit and the p20 magnet.
The electrical unit can generate two different pulses (hereinafter called pulse I and pulse II), as well as I-I, I-II and II-I sequences and a Carr-Purcell sequence. For the sequences the duration between the individual pulses and for the individual pulses the pulse duration can be set. The latter was later adjusted so that the two pulses correspond to a 90° or 180° pulse. The signal generated by the electrical unit is conducted into the magnet, where it generates a magnetic field that deflects the magnetic moments of the atomic nuclei in the sample. These rotate as described in the previous section now with the Larmor frequency and generates a signal with this frequency in an induction coil inside the structure, which is fed back into the electronic unit via the duplexer, where it is modulated with the high-frequency excitation frequency. The resulting signal has an operating frequency which indicates the difference between the excitation frequency and the Larmor frequency. This is displayed on the oscilloscope and read out and evaluated on the PC with LabView.

Determination of relaxation time

Sample	T_1 [ms]	$T_{2,\text{ Spin-echo}}$ [ms]	$T_{2,\text{ Carr-purcell}}$ [ms]
Gd500	190.0 ± 0.6	154.2 ± 0.9	170.1 ± 0.4
Gd600	234.3 ± 0.5	186.5 ± 0.9	198.2 ± 0.7

Table 1: Measured relaxation time

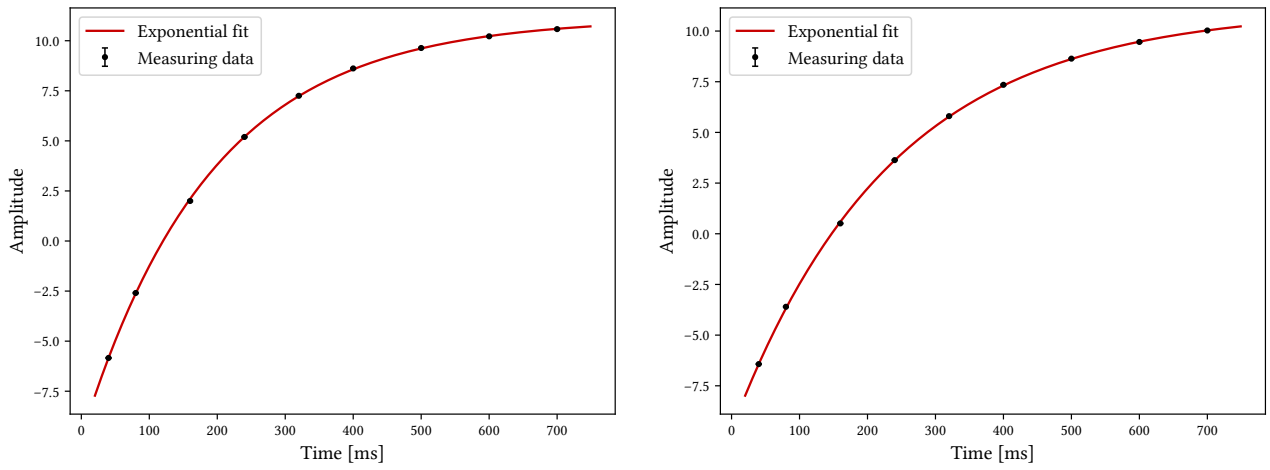

(a) Gd500 (b) Gd600

Figure 6: Results of the measurement for relaxation time T_1

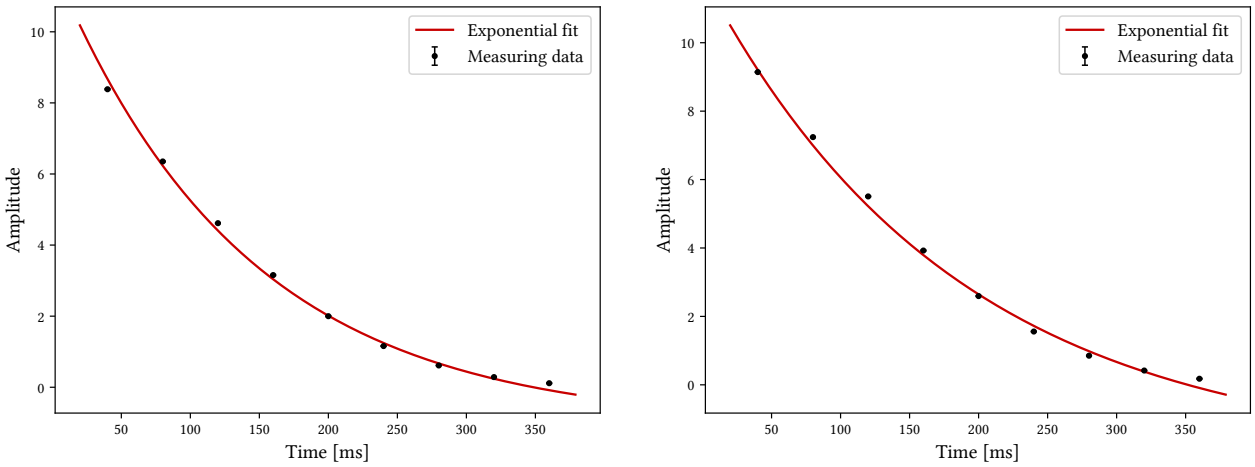

(a) Gd500 (b) Gd600

Figure 7: Results of the measurement for relaxation time T_2 using spin-echo method

Chemical shift

In this part of the experiment we measured the Larmor frequencies of unknown substances with and without the reference substance TMS. This was done by measuring the resonance peaks of the Fourier transform of the registered signal. From the frequency shift measured in this way, the chemical shift can be calculated using equation 9.
Experimentally, we had to give a pulse to the magnet every three seconds and continuously adjust the main magnetic field so that the working frequency is around $\nu_w = 500\,\text{Hz}$. Therefore, one wavelength had to be 2 ms long, which we could achieve via the screw on the magnet.
Table 2 lists the measured chemical shifts of the different samples and their assignment to the corresponding chemical elements. Due to missing samples A,D and E, the shifts could unfortunately

Sample	Shift 1 [ppm]	Shift 2 [ppm]	Shift 3 [ppm]	Substance
A	2.4 ± 0.1	3.9 ± 0.1	6.3 ± 0.1	fluoroacetone
B	2.1 ± 0.1	6.9 ± 0.1		p-xylol
C	9.6 ± 0.1	12.0 ± 0.1		acetic acid
D	4.0 ± 0.1	6.4 ± 0.1		fluoroacetonitril
E	2.2 ± 0.1	7.3 ± 0.1		tuluol

Table 2: Measured chemical shifts

only be taken over by leading test participants.

Now we knew that the elements toluol (CH_3 - C_6H_5), p-xylol (CH_3 - C_6H_4 - CH_3), acetic acid (CH_3 - COOH), fluoroacetone (FCH_2 - CO - CH_3) and fluoroacetonitril (FCH_2 - CN) were among the samples and could classify them according to the same principle with figure 3.
Sample C is the only one that has a shift above 10 ppm and therefore must have a COOH group, which only applies to acetic acid. The two shifts of samples B and E are in fact the same. The same functional groups, a carbon ring and one or two methyl groups for tuluol and p-xylol, cause the same

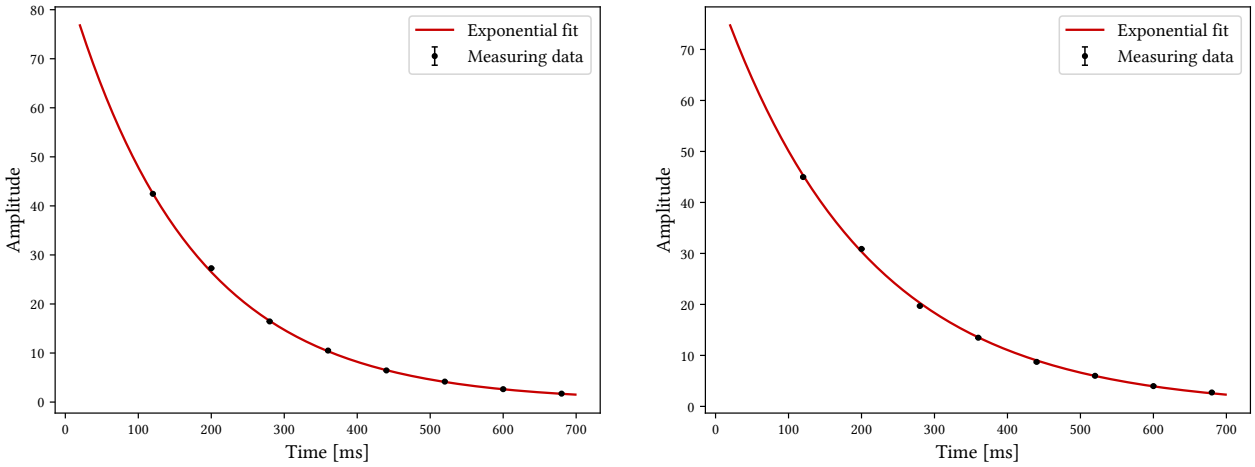

(a) Gd500 (b) Gd600

Figure 8: Results of the measurement for relaxation time T_2 using Carr-purcell sequence

shifts. Because p-xylol contains twice the amount of methyl groups, this substance should show a higher ratio in the peak heights. Sample B shows exactly such a difference and is therefore p-xylol, while sample E is then tuluol. Both fluoroacetone and fluoroacetonitril have a fluoromethyl group and show two identical shifts. Nevertheless, the former has a third shift exactly the same size as tuluol and p-xylol, which could be assigned to the simple methyl group. Therefore, sample A with the additional peak corresponds to fluoroacetone and sample D to fluoroacetonitril.

Imaging techniques

One dimensional imaging

Two dimensional imaging

3. Critical Comment

This experiment was divided into work with a slightly older Bruker minispec p20 spectrometer and a Bruker NMR analyzer mq7.5. First of all, it can be generally said that the older device reacts very sensitively to temperature fluctuations, which is why we often had to readjust the working frequency. Nevertheless, the device was very descriptive and easily accessible from the outside, which makes it a good basis for nuclear magnetic resonance spectroscopy.
In the first part of the experiment we were able to measure the different relaxation times T_1 and T_2 of Gd500 and Gd600 with the device. We found the theoretically expected differences between the times of a sample as well as between the two samples. The times of Gd500 are smaller than those of Gd600 because gadolinium facilitates alignment in the magnetic field. The spin-spin interaction T_2 is less than T_1 becauseIn addition, the times of the spin echo method differ from those of the Carr-purcell method because the spin-echo method gives the sample a certain time to diffuse and the magnetic field can also change during this time.
In the second section we have determined the chemical displacement of various samples. This enabled us to assign functional groups and thus a chemical substance to each sample. The samples

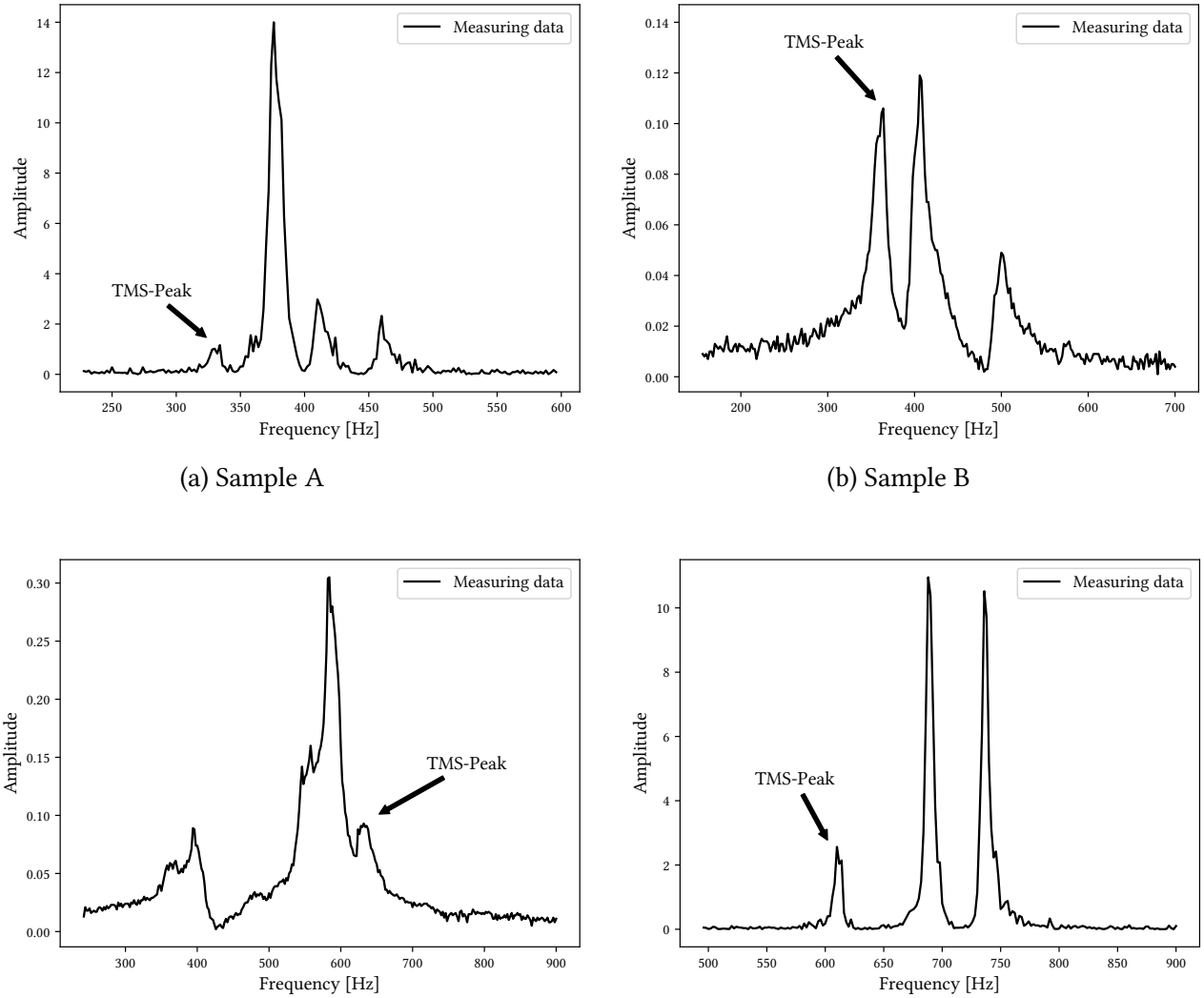

(a) Sample A

(b) Sample B

(c) Sample C

(d) Sample D

Figure 9: Fourier transform of the registered signal

were rotated to compensate for inhomogeneities in the magnetic field. It is noticeable that the magnetic field is shielded differently by different groups, but the assignment by many overlaps is not so clear. This would certainly not be possible without a specification of the possible substances.
Then, using the new NMR analyzer, we used nuclear magnetic resonance spectroscopy for imaging, where the intensity of individual pixels is proportional to the water content. For example, we made one and two dimensional images of some organic and inorganic substances and examined their composition. The correct placement in the analyzer was essential, which quickly became a bit time-consuming. At the end, however, clear structures, such as the air pockets of a peanut, can be seen in the pictures.
Thus, the experiment was very good to gain insights into NMR, which is of course of great importance in medicine.

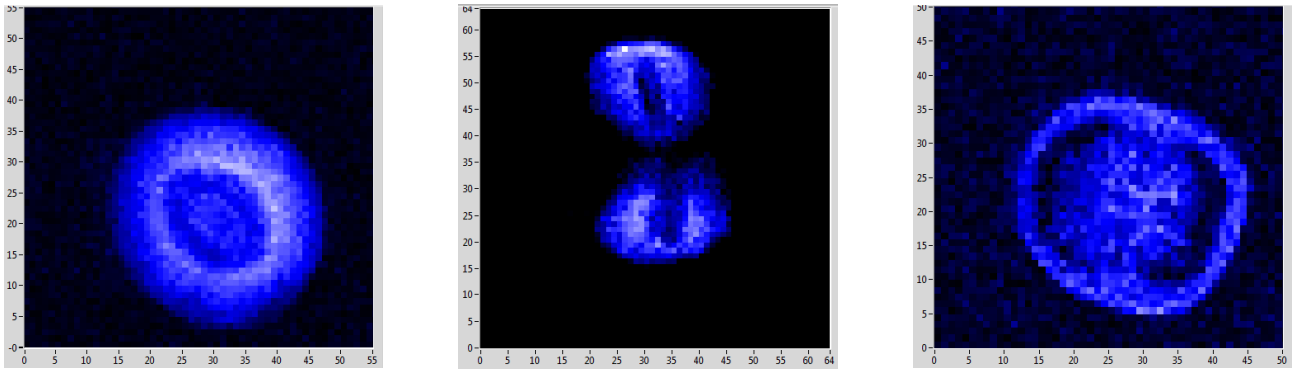

(a) Olive (b) Peanut (c) Chilipepper

Figure 10: Two dimensional NMR imaging

References

[1] R. Schicker. “Nuclear Magnetic Resonance F61/F62. Manual 2.0”. en. In: (Apr. 14, 2010). URL: https://www.physi.uni-heidelberg.de/Einrichtungen/FP/anleitungen/F61.pdf.